ELSEVIER

European Journal of Pharmacology 373 (1999) 223–232

ejp

www.elsevier.nl/locate/ejphar

Propafenone blocks ATP-sensitive K^+ channels in rabbit atrial and ventricular cardiomyocytes

Georges Christé [a,*], Habiba Tebbakh [a], Milena Šimurdová [b], Rémi Forrat [b], Jirí Šimurda [b]

[a] *INSERM U 121, 22 Ave Doyen Lépine, F-69500 Bron, France*
[b] *Department of Physiology, Faculty of Medicine, Masaryk University, Brno, Czech Republic*

Received 10 March 1999; accepted 26 March 1999

Abstract

Propafenone, a class I antiarrhythmic agent, inhibits several membrane currents (I_{Na}, I_{Ca}, I_K, I_{to}), however, its effects on ATP-sensitive potassium current ($I_{K_{ATP}}$) of cardiac cells have not been tested. We evaluated the blocking effects of 0.1 to 100 μM propafenone applications at 35°C on the whole-cell $I_{K_{ATP}}$ as triggered by dinitrophenol (75 μM) in adult rabbit dissociated atrial and ventricular cardiomyocytes in comparison. The block of $I_{K_{ATP}}$ by propafenone was dose-dependent, fully reversible and voltage-independent. The dose–response relation, as evaluated at 0 mV for atrial myocytes ($ED_{50} = 1.26 \pm 0.17$ μM, Hill number $= 1.25 \pm 0.22$) was significantly shifted to the left vs. that in ventricular myocytes ($ED_{50} = 4.94 \pm 0.59$ μM, Hill number $= 1.22 \pm 0.14$). It is concluded that propafenone blocks cardiac $I_{K_{ATP}}$ at a single site with 4 times higher affinity for the drug in atrial myocytes. This block of cardiac $I_{K_{ATP}}$ might play a role in the beneficial and adverse effects of the drug. © 1999 Elsevier Science B.V. All rights reserved.

Keywords: Antiarrhythmic; Propafenone; K^+ channel, ATP-sensitive; Cardiomyocyte; Atrium; Ventricle

1. Introduction

Besides its role in cardioprotection (e.g., Gross and Auchampach, 1992), the outward current through ATP-sensitive K^+ channels (K_{ATP} channels) may be involved in antiarrhythmic (Spinelli et al., 1991) or proarrhythmic actions (Opie, 1993).

A question under debate is whether the effects of individual antiarrhythmic drugs applied to patients with ischemic heart disease might be influenced by their interaction with K_{ATP} channels. Studies on a wide range of antiarrhythmic drugs in rat heart cells (Haworth et al., 1989) and in *Xenopus* oocytes (Sakuta et al., 1992) indicated that some of them are potent blockers of K_{ATP} channels. More detailed data obtained in cardiomyocytes were reported for the effect of lidocaine (Olschewski et al., 1996), the class III agent E-4031 (West et al., 1996) and tedisamil (Németh et al., 1997).

Propafenone is a widely used antiarrhythmic drug known to be effective as a potent inhibitor of fast sodium current (I_{Na}). In agreement with its observed effect on the repolarization phase of action potential (e.g., Delgado et al., 1985), propafenone was recently reported to also inhibit K^+ currents (Duan et al., 1993; Slawsky and Castle, 1994; Delpón et al., 1995;) and Ca^{2+} current I_{Ca} (Delgado et al., 1993; Fei et al., 1993) in concentrations relevant from the viewpoint of therapeutic clinical applications. The effects of propafenone on the main potassium currents occurring under physiological conditions, namely voltage-activated transient outward current (I_{to}), delayed outward current (I_K) and background K current (I_{K1}), were analyzed in detail (Duan et al., 1993). In addition, propafenone was reported to block native K_{ATP} channels in Xenopus oocytes (Sakuta et al., 1992). Surprisingly, the interaction of propafenone with ATP-sensitive potassium channels has not been investigated in cardiac cells.

In the present study, we demonstrate that propafenone effectively and reversibly inhibits $I_{K_{ATP}}$ of rabbit cardiac myocytes in concentrations employed in clinical practice and that $I_{K_{ATP}}$ in atrial myocytes is more sensitive to the drug than in ventricular cells. Accurate $I_{K_{ATP}}$ evaluation revealed that the inhibition is voltage-independent. Prelim-

* Corresponding author. Groupe d'Electrophysiologie Moléculaire, Laboratoire de Bioénergétique Fondamentale et Appliquée, Université Joseph Fourier, B.P. 53 X, F-38041 Grenoble Cedex 9, France. Tel: +33-4-76-51-43-05; Fax: +33-4-76-51-42-18; E-mail: georges.christe@ujf-grenoble.fr

PII: S0014-2999(99)00217-4

inary accounts of these results were published (Christé et al., 1997; Tebbakh et al., 1997).

2. Materials and methods

2.1. Isolation of cardiomyocytes

Conventionally bred New Zealand female rabbits weighting 1.5 to 1.7 kg were used. All steps of the isolation procedure were conducted under sterile conditions. Under deep anesthesia (xylazine 20 mg kg^{-1} plus ketamine 100 mg kg^{-1}), the thorax was opened by sternotomy and the heart was quickly excised and cannulated at the bottom of a Langendorff perfusion system. The heart was rinsed with a well oxygenated, nominally Ca^{2+}-free saline solution (Ca^{+}-free solution) for 10 min under 70 cm water pressure (see Section 2.2 for description of solutions). During this period, 10 mg of collagenase (Yakult YK-101, Tokyo) and 0.5 mg of Sigma type XXIV protease were dissolved in 60 ml of oxygenated Ca^{2+}-free solution. This solution was then recirculated through the heart for 10 min. This was followed by 10 min wash with Ca^{2+}-free solution without enzymes.

The whole right atrium and long strips of the right ventricle were rapidly excised and placed into 250 ml culture flasks with 30 ml fresh Ca^{2+}-free solution under slow horizontal agitation at 37°C. The strips were rinsed twice for 10 min and then exposed to YK-101 collagenase alone (0.33 mg ml^{-1} in Ca^{2+}-free solution). By 30 min, when a large number of myocytes was released, the solution was replaced by HEPES-buffered DMEM medium supplemented with L-glutamine, penicillin, streptomycin and 25 mM glucose (HEPES-DMEM). Shaking was continued until a large density of myocytes was visible. The cell suspension was poured into 50 ml flasks and the heart strips were shaken again with 30 ml of fresh HEPES-DMEM medium for an additional 10 min. Three such agitation periods were performed, both for atrial and ventricular strips.

The cell suspension in the 50 ml flasks was left to sediment in an upright position for 15 min at room temperature. Most of the supernatant was aspirated and cells were resuspended in 10 ml bicarbonate-DMEM. The flasks were then laid horizontal in a culture cabinet (37°C, 5% CO_2 in air saturated with H_2O). The medium was renewed the next day.

2.2. Solutions and pharmacological compounds

All solutions were prepared from non-pyrogenic deionized and distilled water (Laboratoires Aguettant) and were immediately filtered through 0.2 μm cellulose nitrate membranes and stored in sterile glass flasks at 4°C. The nominally Ca^{2+}-free solution contained (mM): NaCl 150; KCl 5.4; $MgCl_2$ 1.2; NaH_2PO_4 0.905; HEPES 10; glucose 10; pH was adjusted to 7.4 with NaOH. The 'external solution' for whole cell experiments was the same solution deprived of NaH_2PO_4 and supplemented with 0.2 mM $CaCl_2$. The pipette solution contained (mM): K-aspartate 115; KCl 5; $MgCl_2$ 7; K_2-ATP 4; Na_2-phosphocreatine 2; pyruvic acid 5; Na_2-EGTA 5; HEPES 10, pH was adjusted to 7.2 with KOH. Concentrations of the Mg-ATP complex and of free Mg^{2+} were estimated to be 3.8 and 2.4 mM, respectively (CHELATOR program, Schoenmakers et al., 1992). Bicarbonate–DMEM was prepared from powder Gibco-Life Sciences Technologies under former catalogue number 52100, its final composition was identical to that of the actual catalogue number 11965, except that the older (cat no. 52100) contained Pyridoxal HCl that is now replaced by an equimolecular amount of Pyridoxine HCl. It was supplemented with penicillin-G 60 mg l^{-1} and streptomycin 50 mg l^{-1}. Its pH was checked to be in the range 7.35 to 7.45 on a 10 ml sample equilibrated for 2 h with 5% CO_2 in air at 37°C in the culture cabinet. HEPES-DMEM medium was prepared in the same way, except that $NaHCO_3$ was replaced by 25 mM HEPES plus 34 mM NaCl for osmotic compensation. Its pH was adjusted to 7.4 with NaOH. It was designed to be used in normal atmosphere.

Pharmacological agents were prepared as stock solutions as follows: 2,4-dinitrophenol (D-7004 Sigma) 20 mM in ethanol; propafenone–HCl (P-4670 Sigma) 1 mM and 10 mM in non-pyrogenic water; glibenclamide (G-106 Research Biochemicals International) 2.5 mM in dimethyl sulfoxide.

2.3. Whole cell recording

Cells were placed in a small (0.5 ml) Perspex chamber whose bottom was made of a glass coverslip. The solution in the chamber was maintained at 35°C by a thermostatted water circulation, and was renewed constantly at 0.5 ml min^{-1}. The solution inlet to the chamber was pre-warmed through a 10 cm water-jacket just before the chamber, the liquid level in the chamber was maintained constant by aspiration.

Cell membrane currents were measured with a List EPC5 patch-clamp amplifier which had been modified to perform whole cell recording: the feedback resistor was changed to a 100 MΩ low noise resistor. Linearity of gain and frequency response were assessed up to ±20 nA and 10 kHz, respectively. Internal low-pass filtering on the current measurement output was permanently adjusted at a cut-off frequency of 3 kHz.

Pipettes were pulled from borosilicate glass (Kavalier, Czech Republic) to resistances ranging 0.7 to 2 MΩ when filled with the internal solution. The bath reference electrode was made of a chlorided silver wire and the pipette holder was equipped with a Ag–AgCl pellet (Clark Medical Instruments). The offset between the two electrodes in the external solution did not exceed 1 mV. Before achiev-

ing whole cell configuration, the offset voltage of the pipette (filled with pipette solution) was compensated to zero.

Once the electrode was sealed to the membrane, the cell became firmly attached to the electrode and it was possible to lift it from the bottom of the chamber in order to place it in front of the outlet of a gravity-driven perfusion inverting system (0.05 ml min^{-1}) that allowed switching to a new solution with a delay of 4 s. Two 0.3 mm ID polyethylene tubes supplied the solution-inverting device. While one solution was steadily flowing over the cell, the other line could be purged with a different solution in a few seconds, which allowed complete flexibility in the sequence of solution changes. This ensured that the medium around the cell was completely renewed. Physical conditions (diameters of outlet tubing and rate of flow) were adjusted so as to mimic conditions tested by Spitzer and Bridge (1989) who brought convincing evidence that this perfusion method can be considered as a quantitatively accurate procedure of changing concentrations around a single cell.

The whole-cell current recording configuration was obtained by breaking the cell-attached membrane patch with a 20 cm water negative pressure briefly applied to the pipette; thereafter, a constant negative pressure of 2 to 5 cm water was maintained during the experiment.

2.4. Data acquisition and processing

A TL1 DA/AD interface and PClamp v5.5 and v6.0 program suites (Axon Instruments) were used for driving and recording. Data processing was done using Clampfit and custom programs in FORTRAN-77 and MATLAB (The Math Works). ORIGIN 4.1 (Microcal) was used for statistical analysis and final graphs.

2.5. Evaluation of dinitrophenol induced current

Our primary aim was to record the $I_{K_{ATP}}$ current under conditions of maximal recruitment of K_{ATP} channels present in a given cell. The use of pharmacological agents to suppress other currents was excluded as to avoid possible interaction with propafenone effects. We also wished to obtain an image of the $I_{K_{ATP}}$ current over a large range of membrane voltages as to detect voltage dependent action of the drug. In a preliminary set of experiments, cell currents were recorded with 200 ms duration step depolarizations from a holding voltage of −80 mV to between −100 and +100 mV in 10 mV increments separated by 5 or 2 s intervals (Fig. 1A). It soon appeared that such a protocol could not be repeated frequently without damage to the cell. Therefore, a ramp-based protocol (Fig. 1B) was used for recording the time-independent dinitrophenol-induced current. It was applied from a holding potential of −80 mV and consisted of a square prepulse to −120 mV for 25 ms, a depolarizing voltage ramp from −120 to +120 mV at 1 mV increment per sample in 96 ms (2.5 mV ms^{-1}) followed by a symmetrical repolarizing voltage

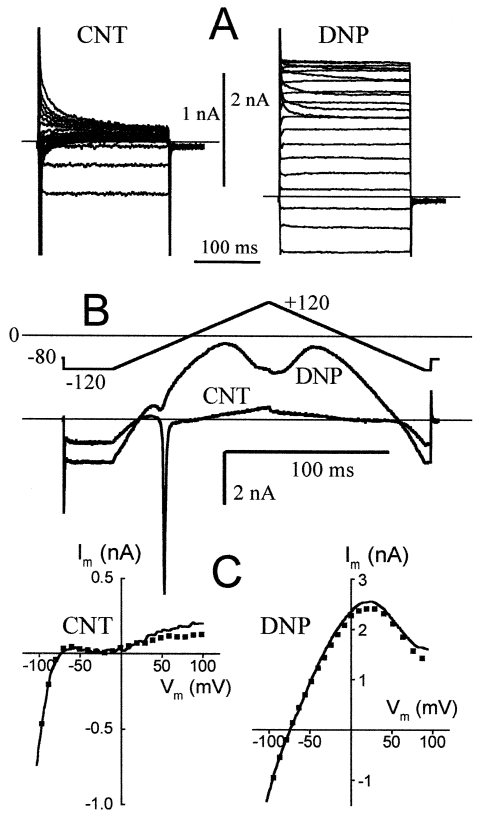

Fig. 1. Comparison of current–voltage relations established in a right ventricular myocyte from rectangular pulses or ramps in control (CNT) and in the presence of 100 μM dinitrophenol (DNP) after appearance of large time-independent current. C_m was 44 pF. (A) current responses to 200 ms square pulses applied from a holding voltage of −80 mV to voltages at −100 mV up to +100 mV in 10 mV increments. Note the different current scaling in CNT and DNP as indicated near the vertical bar. Thin horizontal lines show zero current levels. (B) voltage ramp protocol (upper trace) and superimposed whole cell current response in control and in the presence of DNP (lower traces). (C) comparison of current–voltage relations evaluated from the current responses to rectangular pulses (square dots: currents measured at the end of pulses) and the responses to descending ramps (lines).

ramp. The sampling period was 0.05 ms during the prepulse and 0.4 ms during the ramps. The membrane currents recorded during the repolarizing voltage ramp were used for data analysis. The pulse-and-ramps voltage protocol was imposed at 20 s intervals during a whole experiment. The adequacy of the ramp paradigm was assessed in a preliminary series ($n = 7$) in comparison with the classical pulse method, as exemplified in Fig. 1C.

In control Tyrode solution (trace CNT in Fig. 1B), the current response to the depolarizing ramp initially displayed the inward rectifying I_{K1} current with an abrupt inward current superimposed upon the region of inward rectification. This inward peak exhibited properties of fast Na^+ current I_{Na}, i.e., it was almost completely suppressed by 10^{-5} M tetrodotoxin or by changing the holding command voltage from −80 to −65 mV (not shown). During the repolarizing ramp, I_{Na} had been completely inacti-

vated. Ca^{2+} current I_{Ca} was low due to the low concentration of $CaCl_2$ (0.2 mM) in the external solution and its time course was slow as compared to the huge rapid inward transient. Due to the capacitive current, a small positive offset appeared in response to the depolarizing ramp and a small negative offset in response to the repolarizing ramp. The outward current during the second half of the depolarizing ramp and the first half of the repolarizing ramp may be influenced by time-dependent potassium currents, namely by the transient outward currents I_{to} and delayed outward current I_K (see Section 4 for the estimate of the effects of control current components on the present results).

Current–voltage relations were constructed from data acquired during the repolarizing voltage ramp. The presentation of experimental data use the current and voltage values obtained after correction for junction potentials, series resistance, and cell capacitive current. The correction was based on the same principles as used in on-line corrections. The real membrane voltage differs from the command voltage by a voltage drop across series resistance R_s due to the flow of membrane current I_m. This, however, does not introduce ambiguity to the evaluated current–voltage relation because $I_{K_{ATP}}$ is time-independent. Thus, its current voltage relation does not depend on the time course of the testing membrane voltage. The voltage drop $I_m R_s$ and the calculated junction potential (P.H. Barry's JPCalc subprogram of AxoScope, Axon Instruments) were subtracted from the command voltage to obtain the true value of membrane voltage V_m. The first time derivative dV_m/dt was evaluated numerically from a 7th order polynomial fit of V_m vs. time. The capacitance current $C_m dV_m/dt$ was then subtracted from I_m. The values of R_s and C_m were evaluated by analyzing the exponential time course of relaxation of the capacitive current during the prepulse from the holding potential of -80 mV to -120 mV. The final relative error on V_m and I_m were estimated to remain within 5%, as assessed from a Monte Carlo evaluation of errors on R_s and C_m evaluations with a Gaussian noise level similar to that found in our recordings.

The final dinitrophenol-induced current was evaluated after subtraction of the whole cell current recorded in the absence of dinitrophenol.

To represent the time-course of changes in dinitrophenol-induced current during an experiment, the current at one or several voltages were extracted from each current voltage relation and plotted as a function of the time of protocol application.

Statistical results were expressed as mean ± S.E.M. and significance of differences was evaluated with $p < 0.05$.

2.6. Monitoring of the cell image

One of the effects of prolonged dinitrophenol exposure was a contracture of the examined cell. To indicate the time of contracture development the image of the cell was continuously monitored on the video display from the camera mounted on the microscope.

3. Results

3.1. Characteristics of the dinitrophenol-induced outward current

Each myocyte was allowed to stabilize for 10 min in control Tyrode solution after the formation of the whole-cell current recording configuration before exposure to dinitrophenol. The time delay to the onset of the dinitrophenol-induced conductance varied considerably from myocyte to myocyte (20 s to 20 min). The effect of dinitrophenol was progressive and preceded by 1 to 10 min the development of a poorly reversible contracture observed on continuously monitored image of the cell. Fig. 2A shows results of a representative experiment. The time of contracture development is indicated by the asterisk on the zero current line. The washout of dinitrophenol caused the almost immediate loss of the dinitrophenol-induced current. The reintroduction of dinitrophenol then provoked an increase in cell current which reached a maximum in less

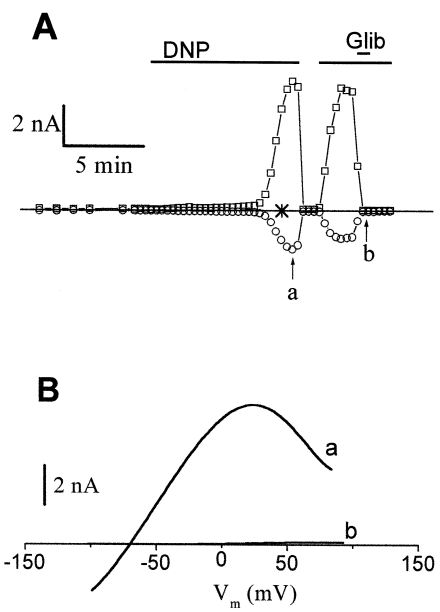

Fig. 2. The DNP-induced current is reversible and sensitive to glibenclamide. (A) Response of a ventricular myocyte to 75 μM DNP applied for the periods indicated by the bars above the graph, at two voltage values: 0 mV (squares) and −90 mV (circles). Plotted currents represent deviation from control currents recorded just before application of DNP. Ten μM glibenclamide (Glib) was applied in the continuous presence of DNP. The asterisk upon the zero current line shows the time when the cell became fully contractured. (B) Superimposed current–voltage relations for the DNP induced current as recorded at two instances: (a) at maximal DNP-induced current during the first exposure and (b) in the presence of 10 μM glibenclamide and DNP. The corresponding times to (a, b) are indicated by the arrows in panel A.

than 60 s. Glibenclamide (10 μM) blocked the membrane current induced by dinitrophenol by 98%. The dinitrophenol-induced current displayed a strong inward rectification with a negative slope at voltages beyond +30 mV (Fig. 2B).

These features identify the dinitrophenol-induced current as the glibenclamide-sensitive $I_{K_{ATP}}$ current currently observed in cardiac myocytes (e.g., Noma, 1983; Findlay, 1987). In Fig. 2A it may be seen that 7 min after the cell had been in full contracture the dinitrophenol-induced current was still fully blocked by 10 μM glibenclamide. This was true for the cells that had been in contracture for up to 20 min (not shown). In this respect, the rabbit ventricular cells differ from the adult rat cardiomyocytes, which were shown to loose sensitivity to glibenclamide under conditions of severe metabolic impairment (Findlay, 1992; Krause et al., 1995).

The rundown of current under metabolic poisoning (Deutsch and Weiss, 1993) was absent in about half of the cells. This unusual stability of $I_{K_{ATP}}$ may be due to the large concentration of Mg-ATP in our pipette solution (Findlay and Dunne, 1986) supporting the phosphorylated state of the K_{ATP} channels (Furukawa et al., 1994). The presence of creatine phosphate and a physiological temperature (35°C) may also have been able to support effective phosphorylation of the K_{ATP} channel.

The inward rectification depends strongly on the intracellular concentration of Mg^{2+} (Horie et al., 1987; Takano and Noma, 1993). Increasing $[Mg^{2+}]_i$ results in more prominent rectification and in a shift (towards less positive values) of the voltage at which $I_{K_{ATP}}$ starts to decline. In our experiments, $[Mg^{2+}]_i$ was estimated at 2.4 mM and $I_{K_{ATP}}$ reached its maximum at around +30 mV. This is in line with quantitative considerations of Horie et al. (1987) and prediction of the rate theory model for Mg^{2+} block of $I_{K_{ATP}}$ (Davies et al., 1996).

3.2. Effects of propafenone on $I_{K_{ATP}}$

3.2.1. Reversibility of inhibitory effect

After activation of $I_{K_{ATP}}$ by the superfusion of dinitrophenol the cells were exposed to propafenone in progressively increasing concentrations (Fig. 3A). A wash period was interposed between successive applications of the drug in order to assess the reversibility of the block and the stability of the $I_{K_{ATP}}$ current. Voltage ramp protocols were applied at 20 s intervals during the whole experiment. The block of $I_{K_{ATP}}$ by propafenone was completely reversible, even for the largest dose of 100 μM. This was found in all the myocytes studied.

3.2.2. Voltage independence

The ramp protocol made it possible to follow changes of current–voltage relation in the course of experiment. Results obtained at fully developed dinitrophenol-induced current and at steady-state effect of propafenone in concentrations indicated in Fig. 3A are shown in Fig. 3B. The similar shape of all curves suggests the same blocking effect at all voltages. As documented in Fig. 3C, it is really the case. Here the propafenone-blocked fraction of $I_{K_{ATP}}$ is plotted against membrane voltage. The inhibitory action of the drug is completely voltage independent at all of the concentrations tested. Similar conclusions were drawn from

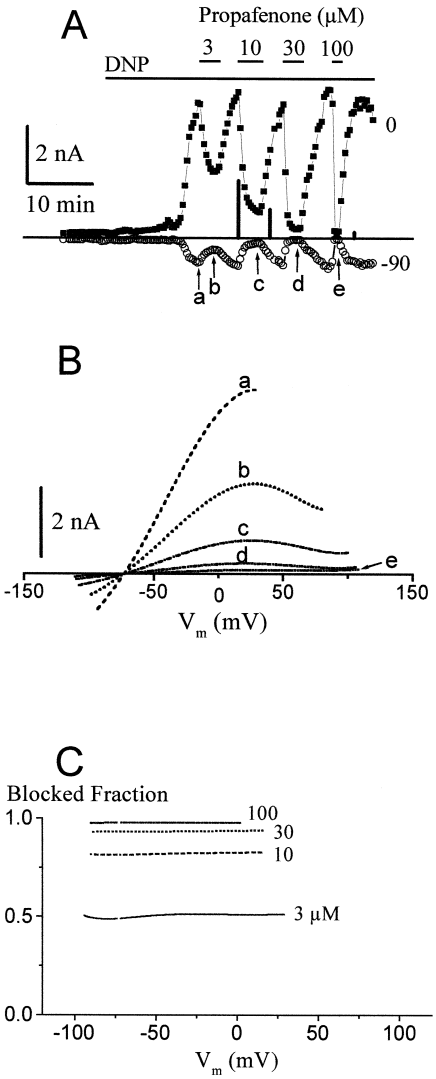

Fig. 3. Propafenone block of $I_{K_{ATP}}$ was dose-dependent, reversible and voltage independent. (A) Changes in the $I_{K_{ATP}}$ current in response to the addition and washout of different concentrations of propafenone at the times indicated by the bars above the graph. Current values taken at 0 mV (squares) and at −90 mV (circles) were plotted along time. The vertical bars upon the zero current line show the relative length of the cell, which had remained fully elongated up to the time of the first bar (full length). (B) Current–voltage relations obtained at the times indicated by the arrows in A. (a) maximal DNP-induced current; (b) to (e) respectively in the presence of 3, 10, 30 and 100 μM propafenone. (C) Voltage independent block of $I_{K_{ATP}}$ by propafenone. The fraction of blocked current was computed for each voltage as the ratio of the current blocked by the presence of propafenone to current recorded prior to the application of the drug (in concentrations 3, 10, 30 and 100 μM). Data taken from the same myocyte as in A and B.

the analysis of data from 6 other ventricular and atrial myocytes.

3.2.3. Kinetics of block

Fig. 4 shows superimposed time courses of block development and recovery from block in response to exposure to propafenone in concentrations of 3, 10 and 30 μM and following washouts. Results are taken from the representative experiment presented in Fig. 3. The response to 100 μM concentration was omitted because the onset of block was too fast with regard to the sampling period of 20 s. After addition of propafenone, $I_{K_{ATP}}$ declined towards a steady level following approximately a single exponential function while responses to washout exhibited delay. This behaviour complies with an idea that propafenone has direct access to its binding site from extracellular medium and, in addition, from an internal pool that is gradually built up and depleted during washout periods. Following this notion, the time courses of onset of block were approximated with single exponentials while the recoveries from block were fitted with solutions of a first-order differential equation describing decrease of block under the assumption that the pool of active drug is gradually exhausted following a monoexponential time course.

3.2.4. Dose response

Concentration-dependent effect of propafenone on $I_{K_{ATP}}$ was analyzed at 0 mV in 10 atrial myocytes from 6 different rabbits and 9 ventricular myocytes from 3 rabbits. Each cell was subjected to from 1 to 4 different concentrations of propafenone, separated by a wash period until full recovery from block was obtained (as illustrated in Fig. 4). Data were evaluated as the ratio of the propafenone-sensitive current to the maximal current evoked by DNP immediately before the application of the drug. The data points in Fig. 5 represent 28 measurements in the atrial cells and 21 measurements in the ventricular cells. The solid lines represent the results of a least-squares fit to the data using the equation:

$$\frac{I_{con} - I_p}{I_{con}} = \frac{[P]^h}{IC_{50}^h - [P]^h} \quad (1)$$

where I_{con} and I_P are currents measured at 0 mV before and after the application of propafenone, respectively. $[P]$ is the concentration of propafenone and ED_{50} is the concentration required for half-maximal inhibition. This analysis provided an ED_{50} of 1.26 (±0.17) μM and a Hill number h of 1.25 (±0.22) in atrial cells, and an ED_{50} of 4.94 (±0.59) μM and Hill number of 1.22 (±0.14) in ventricular cells. Numbers in parentheses refer to the 95% confidence limit as computed by the fitting routine (Levenberg–Marquardt algorithm in Origin 4.1).

Two tests were used to evaluate the difference between the ED_{50} values obtained from atrial and ventricular myocytes. A t-test was applied using the number of data and the confidence limits to evaluate the common variance. This yielded the conclusion that ED_{50}'s were different,

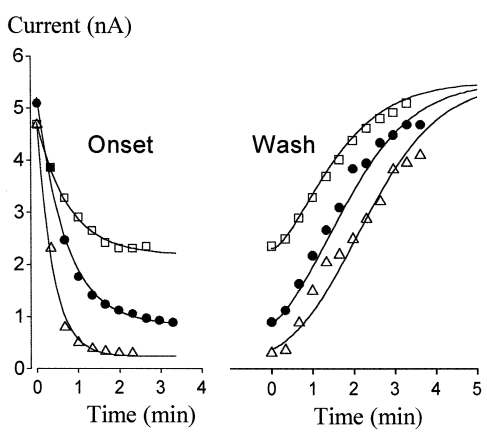

Fig. 4. The superimposed time courses of propafenone action on the DNP-induced current (from Fig. 3A) measured at 0 mV. The onset and the washout of drug action were followed in response to applications of concentrations of 3 μM (open squares), 10 μM (filled circles) and 30 μM (open triangles). The onset of block was fitted using a single exponential function $I = I_\infty + (I_o - I_\infty)\exp(-t/\tau_{on})$ where τ_{on} is the time constant (0.77, 0.70, and 0.38 min for concentrations 3, 10 and 30 μM, respectively), I_0 and I_∞ are initial and steady-state currents. The recoveries from drug action were fitted to solutions of differential equation $\tau_{off}\frac{dI}{dt} + I(\frac{I_\infty - I_0}{I_0}\exp(-t/\tau_d) + I_\infty) - I_\infty = 0$ The values of constants were: $\tau_{off} = 0.8$ min, $\tau_d = 0.7$ min, $I_\infty = 5.5$ nA and $I_0 = 2.31$, 0.9, and 0.38 nA for 3, 10, and 30 μM concentration of propafenone, respectively.

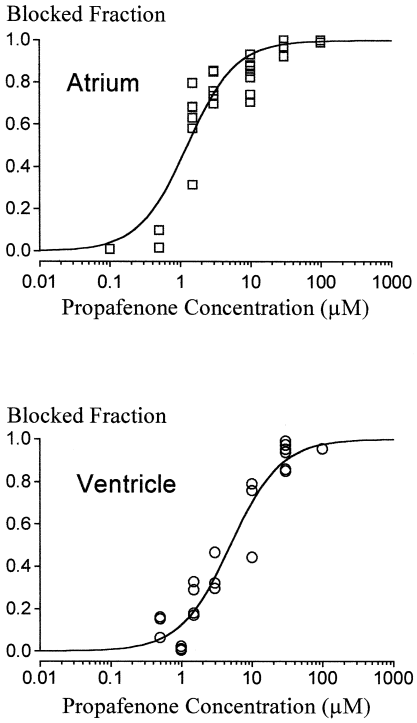

Fig. 5. Dose–response analysis of the effects of propafenone on $I_{K_{ATP}}$ current. Individual measurements of the blocked fraction in the presence of a single dose of propafenone were pooled for atrial and ventricular myocytes respectively. Each data set was fitted (solid line) with Eq. (1).

with $p < 0.01$. In another test, the theoretical values of the parameters of the equation fitted to a given data set served to compute theoretical data points at all abscissas corresponding to the other experimental data set. A paired *t*-test was then performed for the ability of the parameters for a given model to represent the other data series. In both combinations, i.e., for the ventricular model to account for the atrial data and vice-versa, the hypothesis of a difference received a risk p value < 0.001 (analyzed using the BMDP software). There was no significant difference in the Hill numbers of atrial and ventricular data, neither were they significantly different from unity.

4. Discussion

4.1. Accuracy of measurement of $I_{K_{ATP}}$ sensitivity to propafenone

The level of propafenone induced block of $I_{K_{ATP}}$ was evaluated from the sensitivity to the drug of maximum current recorded under the effect of dinitrophenol. This current also included, besides the dominant $I_{K_{ATP}}$, the background current I_{K1} and partially activated time dependent components, namely I_{Ca}, I_{to} and I_K. All these currents were shown to be inhibited by propafenone though in different degrees (see Section 4.4). The error in evaluation of the fraction of blocked K_{ATP} channels due to the minor current components depends first, on the ratio of the control current recorded in Tyrode solution to $I_{K_{ATP}}$ and second, on the difference between sensitivities of both currents to propafenone. At 0 mV of membrane voltage (at which the dose responses of $I_{K_{ATP}}$ (Fig. 5) were evaluated), the sum of control currents did not exceed 4% of the dinitrophenol induced current (Fig. 1C). Even though the ED_{50} of the total control current differed by one order from the ED_{50} of $I_{K_{ATP}}$ the error in evaluation of the fraction of blocked K_{ATP} channels would not exceed 2%. In the whole range of tested membrane voltages the estimate of maximum error amounts 5%.

4.2. The effect of dinitrophenol

It can be argued that the opening of K_{ATP} channels in our experiments might result from direct action of dinitrophenol on K_{ATP} channels rather than from a lack of ATP. Alekseev et al. (1997) described dinitrophenol (200 μM) induced activity of K_{ATP} channels insensitive to both $[ATP]_i$ and the specific inhibitor glibenclamide (10 μM). It was proposed that the loss of sensitivity may be associated with disturbances of the regulatory gating of K_{ATP} channel. The following observations indicate that such a direct effect (if any) would be only of marginal significance in our experiments: (1) As demonstrated in Fig. 2A, $I_{K_{ATP}}$ was completely blocked by 10 μM glibenclamide. (2) The appearance of $I_{K_{ATP}}$ under the effect of dinitrophenol was regularly followed (with a delay) by a cell contracture due to ATP insufficiency. (3) Some of the adult rabbit ventricular cells used here developed spontaneously a large inward rectifying current with properties identical to those of the dinitrophenol-induced current (i.e., huge current density, completely blocked by 10 μM glibenclamide, reversal voltage around −75 mV, shallow inward rectifier shape of I/V curve at voltages above 0 mV). We observed similar potency of propafenone on this current. Spontaneously developed currents during long whole cell recording having properties of $I_{K_{ATP}}$ were described by Belles et al. (1987) in guinea pig ventricular myocytes. (4) In our experiments, the exposure to dinitrophenol lasted up to 20 min before the KATP current appeared. An average delay of 13 min was observed for action potential shortening in response to hypoxia (Shigematsu and Arita, 1997). This may be related to the time needed to achieve conditions for the activation of K_{ATP} channels (probably a decrease of the ATP/ADP ratio in the vicinity of the K_{ATP} channels). Such a delay is hardly to expect if dinitrophenol opened K_{ATP} channels directly.

4.3. Comparison of the effect of propafenone on $I_{K_{ATP}}$ in atrial and ventricular cells

The difference in sensitivity between atrial and ventricular cells is significant. On average, the $I_{K_{ATP}}$ of atrial myocytes is 4 times more sensitive to block by propafenone than in ventricular myocytes. On the other hand, in both cell types a Hill number near unity was estimated for the block of $I_{K_{ATP}}$ by propafenone, indicating that a single molecule would bind to each ion channel.

4.4. Comparison of the effect of propafenone on $I_{K_{ATP}}$ and other currents

The propafenone effect on $I_{K_{ATP}}$ is reversible even after complete block induced by 100 μM concentration (Fig. 3). In contrast, no recovery was observed after inhibition of I_{Ca} by 50 μM propafenone (Delgado et al., 1993).

The values of half-maximal block by propafenone for individual ionic current components as reported by different authors diverge considerably, apparently due to various experimental conditions and to use-dependent features of block of I_{Na} (Kohlhardt and Seifert, 1980), I_{Ca} (Delgado et al., 1985) and I_K (Delpón et al., 1995). Nevertheless, all values fall in a relatively narrow range between 0.75 and 10 μM (Delgado et al., 1985; Honjo et al., 1989; Duan et al., 1993; Fei et al., 1993; Delpón et al., 1995). The block of $I_{K_{ATP}}$ with ED_{50}'s of 1.3 μM (atrial cells) and 4.9 μM (ventricular cells) fits into this range and suggests relatively high affinity of propafenone to K_{ATP} channels. The action of propafenone on I_{Na} differs largely from that on I_{KATP}, in that the tonic block of I_{Na} shows strong voltage dependence and a Hill number of 1.76 (Kohlhardt, 1984).

Propafenone is thus likely to act by different mechanisms on different channels.

4.5. Voltage-independence of propafenone's action on $I_{K_{ATP}}$

Propafenone is a highly protonated molecule ($pK_a > 9$) existing in more than 95% charged form at physiological pH. Since the level of block was independent of membrane voltage (Fig. 3C) block from the bulk medium in the protonated form at any non-zero distance within the electrical field in the K_{ATP} channel or a regulatory cofactor can be excluded. Propafenone could act in the charged form strictly out of the transmembrane electric field, or in the uncharged form, likely in a hydrophobic region of the membrane channel or regulatory molecule.

Another consequence of the constant fraction of blocked current vs. voltage is that the observed strong inward rectification (Fig. 3B) was not influenced by propafenone; the current–voltage relation in various concentrations is constant in shape to within a multiplying factor. Thus, the interaction of the channels with the main determining factors of inward rectification, namely internal magnesium ions (Findlay, 1987; Horie et al., 1987) and polyamines (Niu and Meech, 1998) was not changed by propafenone.

Extracellular accumulation of potassium ions at large current densities (Yasui et al., 1993; Tourneur et al., 1994), should be less prominent when the major part of the current is suppressed. If this phenomenon would be effective, an increase of the K_{ATP} channel conductance should distort the current–voltage relation, and cause apparent voltage dependency, which is not seen.

Voltage dependent action has been documented for the effects of antiarrhythmics disopyramide and quinidine upon $I_{K_{ATP}}$ with a stronger block at depolarized voltages in cat ventricular myocytes. The site was located respectively at 0.48 and 0.51 fractional distance in the transmembrane electric field from the inner mouth of the channel (De Lorenzi et al., 1995). A weak voltage dependence was observed for cibenzoline (Horie et al., 1992). This is in contrast with the voltage independence of block by propafenone (Fig. 3).

4.6. Comparison with other antiarrhythmic agents

Several antiarrhythmic agents cause hypoglycemia that is likely due to their ability to block K_{ATP} channels in pancreatic β-cells (Horie et al., 1992; Kakei et al., 1993). The same agents (cibenzoline and disopyramide: Horie et al., 1992; cibenzoline: Sato et al., 1993) and other antiarrhythmics have been reported to inhibit cardiac $I_{K_{ATP}}$ current triggered by metabolic impairment in adult animal cardiac cells (Wu et al., 1992; Olschewski et al., 1996). Also, tedisamil is efficient in reversing the shortening of cardiac action potential duration due to hypoxia (Németh et al., 1997). The ED_{50} and Hill number (h) for cibenzoline and disopyramide in their blocking effect on cardiac $I_{K_{ATP}}$ were, respectively, 0.9 μM ($h = 1.3$) and 1.8 μM ($h = 1.0$) in rat ventricular myocytes (Horie et al., 1992). In cat ventricular myocytes disopyramide and quinidine had respective ED_{50}'s of 4.6 and 1.5 μM (De Lorenzi et al., 1995), while ED_{50} for quinidine in rat ventricular myocytes was 2.7 μM (Haworth et al., 1989). Thus, propafenone, with ED_{50}'s of 1.3 and 4.9 μM respectively in atrial and ventricular myocytes, appears to be among the most potent antiarrhythmic agents tested on cardiac K_{ATP} channels activated under similar conditions.

Surprisingly, some antiarrhythmic agents are able to activate $I_{K_{ATP}}$. Mexiletine, a class Ib agent, applied at 100 μM was able to shorten the action potential of guinea-pig papillary muscle and to increase K_{ATP} channel open probability in inside-out patches (Sato et al., 1995). However, mexiletine was found to be a weak inhibitor of *Xenopus* oocyte KATP current with $ED_{50} = 63.1$ μM (Sakuta et al., 1992). In the present study, we did not observe any activating effect of propafenone when applied in the control Tyrode solution at concentrations of from 5 μM to 100 μM. These diverse actions of antiarrhythmic compounds are likely due to interaction with different binding sites (Benz and Kohlhardt, 1994).

4.7. Clinical relevance

The available data of numerous clinical studies and trials clearly suggest that propafenone is effective and relatively safe in pharmacological suppression of supraventricular arrhythmias, mainly atrial fibrillation, in adults and children (Kishore and Camm, 1995). On the other hand, a serious warning follows from clinical experience against the employment of propafenone in patients with significant ischemic heart diseases (Capucci and Boriani, 1995). The present results suggest that the adverse effect of propafenone on ischemic heart might be at least partly related to suppression of natural protective effect of K_{ATP} channels activation. The results of Electrophysiological Study Versus Electrocardiographic Monitoring (ESVEM) trial (Mason, 1993) seem to support this view. During a 1-year follow-up, the risk of death from cardiac conditions were significantly lower in sotalol-treated group than in patients tested with other drugs including propafenone. Comparison of the inhibitory effects of various antiarrhythmic agents (representatives of classes I–IV) in frog oocytes have shown that the sensitivity of K_{ATP} current to propafenone was by two orders higher than that to sotalol (Sakuta et al., 1992). Relatively low sensitivity of K_{ATP} channels to sotalol (with IC_{50} of 43 μM) was confirmed also in single channel experiments in neonatal rat cardiac myocytes (Benz and Kohlhardt, 1994). The involvement of K_{ATP} channels in cardioprotection induced by ischemic preconditioning was evidenced in a clinical study by Tomai et al. (1994).

The present results show that in rabbit cardiomyocytes the blocking potency of propafenone is relatively high. A

question arises if it is high enough in men to be significant in clinical applications. The results of comparative studies have shown that the maximal amplitude of $I_{K_{ATP}}$ reached under hypoxia or dinitrophenol is less in human than in rabbit myocytes (Veldkamp et al., 1995; Verkerk et al., 1996). Even though the results from human myocytes were obtained from diseased hearts, significant species differences in density or open state probability of K_{ATP} channels and also in sensitivity to antiarrhythmic drugs are likely. Therefore, the following considerations must be regarded only tentative.

According to the estimation of Duan et al. (1993), approximate in-vitro concentrations of propafenone corresponding to clinically effective free drug concentrations are probably between 0.2 and 0.6 μM. In a clinical study, Keller et al. (1978) found that the peak serum concentration after a single oral dose of 900 mg was about 5 μM after 2 h. At this concentration, in the present study, 80% and 50% of $I_{K_{ATP}}$ were blocked in atrial and ventricular myocytes, respectively (Fig. 5). However, much higher concentrations of propafenone may be reached and adverse effects of the drug may occur when administered to a poor metabolizer of the molecule which is the case in about 7% of Europeans and 10% of North Americans (Bryson et al., 1993). Moreover, the antiarrhythmic activity and adverse effects do not correlate adequately with plasma concentrations because of the contribution of active metabolites (Capucci and Boriani, 1995).

It can be concluded that during an ischemic episode the block of $I_{K_{ATP}}$ by propafenone is likely to be clinically relevant. This conclusion warrants more experimental work to be done on the side effects of antiarrhythmic drugs in relation to their inhibitory action on ATP-dependent potassium current in man.

Acknowledgements

The authors are grateful to Dr. Ian Findlay for critical reading and helpful suggestions during the elaboration of this manuscript. Their thanks go to Mr. Aimé Toullier for technical support. M. Šimurdová and J. Šimurda are supported by grant GA CR 305/97/0043 of the Czech Granting Agency.

References

Alekseev, A.E., Gomez, L.A., Aleksandrova, L.A., Brady, P.A., Terzic, A., 1997. Opening of cardiac sarcolemmal KATP channels by dinitrophenol separate from metabolic inhibition. J. Membr. Biol. 157, 203–214.

Belles, B., Hescheler, J., Trube, G., 1987. Changes of membrane currents in cardiac cells induced by long whole-cell recordings and tolbutamide. Pflügers Arch. 409, 582–588.

Benz, I., Kohlhardt, M., 1994. Distinct modes of blockade in cardiac ATP-sensitive K^+ channels suggest multiple targets for inhibitory drug molecules. J. Membr. Biol. 142, 309–322.

Bryson, H.M., Palmer, K.J., Langtry, H.D., Fitton, A., 1993. Propafenone. A reappraisal of its pharmacology, pharmacokinetics and therapeutic use in cardiac arrhythmias. Drugs 45, 85–130.

Capucci, A., Boriani, G., 1995. Propafenone in the treatment of cardiac arrhythmias. A risk-benefit appraisal. Drug Safety 12, 55–72.

Christé, G., Simurdova, M., Tebbakh, H., Forrat, R., Simurda, J., 1997. Therapeutic levels of antiarrhythmic propafenone inhibit ATP-sensitive channels in rabbit myocardial cells. Physiol. Res. 46, 9 pp. (Abstract).

Davies, N.W., McKillen, H.C., Stanfield, P.R., Standen, N.B., 1996. A rate theory model for Mg^{2+} block of ATP-dependent potassium channels of rat skeletal muscle. J. Physiol. (London) 490, 817–826.

De Lorenzi, F.G., Bridal, T.R., Spinelli, W., 1995. Voltage-dependent inhibition of the ATP-sensitive K^+ current by the class Ia agent disopyramide in cat ventricular myocytes. J. Pharmacol. Exp. Ther. 272, 714–723.

Delgado, C., Tamargo, J., Tejerina, T., 1985. Electrophysiological effects of propafenone in untreated and propafenone pretreated guinea-pig atrial and ventricular muscle fibers. Br. J. Pharmacol. 86, 765–775.

Delgado, C., Tamargo, J., Henzel, D., Lorente, P., 1993. Effects of propafenone on calcium current in guinea-pig ventricular myocytes. Br. J. Pharmacol. 108, 721–727.

Delpón, E., Valenzuela, C., Perez, O., Casis, O., Tamargo, J., 1995. Propafenone preferentially blocks the rapidly activating component of delayed rectifier K^+ current in guinea pig ventricular myocytes. Voltage-independent and time-dependent block of the slowly activating component. Circ. Res. 76, 223–235.

Deutsch, N., Weiss, J.N., 1993. ATP-sensitive K^+ channel modification by metabolic inhibition in isolated guinea-pig ventricular myocytes. J. Physiol. (London) 465, 163–179.

Duan, D., Fermini, B., Nattel, S., 1993. Potassium channel blocking properties of propafenone in rabbit atrial myocytes. J. Pharmacol. Exp. Ther. 264, 1113–1123.

Fei, L., Gill, J.S., McKenna, W.J., Camm, A.J., 1993. Effects of propafenone on calcium currents in single ventricular myocytes of guinea-pig. Br. J. Pharmacol. 109, 178–182.

Findlay, I., 1987. ATP-sensitive K^+ channels in rat ventricular myocytes are blocked and inactivated by internal divalent cations. Pflügers Arch. 410, 313–320.

Findlay, I., 1992. Sulphonylurea drugs no longer inhibit ATP-sensitive K^+ channels during metabolic stress in cardiac muscle. J. Pharmacol. Exp. Ther. 266, 456–467.

Findlay, I., Dunne, M.J., 1986. ATP maintains ATP-inhibited K^+ channels in an operational state. Pflügers Arch. 407, 238–240.

Furukawa, T., Virag, L., Furukawa, N., Sawanobori, T., Hiraoka, M., 1994. Mechanism for reactivation of the ATP-sensitive K^+ channel by MgATP complexes in guinea-pig ventricular myocytes. J. Physiol. (London) 479, 95–107.

Gross, G.J., Auchampach, J.A., 1992. Blockade of ATP-sensitive potassium channels prevents myocardial preconditioning in dogs. Circ. Res. 70, 223–233.

Haworth, R.A., Goknur, A.B., Berkoff, H.A., 1989. Inhibition of ATP-sensitive potassium channels of adult rat heart cells by antiarrhythmic drugs. Circ. Res. 65, 1157–1160.

Honjo, H., Watanabe, T., Kamiya, K., Kodama, I., Toyama, J., 1989. Effects of propafenone on electrical and mechanical activities of single ventricular myocytes isolated from guinea-pig hearts. Br. J. Pharmacol. 97, 731–738.

Horie, M., Irisawa, H., Noma, A., 1987. Voltage-dependent magnesium block of adenosine triphosphate-sensitive potassium channels in guinea-pig ventricular cells. J. Physiol. (London) 387, 251–272.

Horie, M., Hayashi, S., Yousuke, Y., Sasayama, S., 1992. Comparative studies of ATP sensitive potassium channels in heart and pancreatic β cells using Vaughan–Williams class Ia antiarrhythmics. Cardiovasc. Res. 26, 1087–1094.

Kakei, M., Nakazaki, M., Kamisaki, T., Nagayama, I., Fukamashi, Y., Tanaka, H., 1993. Inhibition of the ATP-sensitive potassium channel by class I antiarrhythmic agent, cibenzoline, in rat pancreatic β-cells. Br. J. Pharmacol. 109, 1226–1231.

Keller, K., Meyer-Estorf, G., Beck, O.A., Hochrein, H., 1978. Correlation between serum concentration and pharmacological effect on atrioventricular conduction time of the antiarrhythmic drug propafenone. Eur. J. Clin. Pharmacol. 13, 17–20.

Kishore, A.G.R., Camm, A.J., 1995. Guidelines for the use of propafenone in treating supraventricular arrhythmias. Drugs 50, 250–262.

Kohlhardt, M., 1984. Block of sodium current by antiarrhythmic agents: analysis of the electrophysiologic effects of propafenone in heart muscle. Am. J. Cardiol. 54, 13D–19D.

Kohlhardt, M., Seifert, C., 1980. Inhibition of V_{max} of the action potential by propafenone and its voltage-, time- and pH-dependence in mammalian ventricular myocardium. Arch. Pharmacol. 315, 55–62.

Krause, E., Englert, H., Gogelein, H., 1995. Adenosine triphosphate-dependent K currents activated by metabolic inhibition in rat ventricular myocytes differ from those elicited by the channel opener rilmakalim. Pflügers Arch. 429, 625–635.

Mason, J.W., 1993. A comparison of seven antiarrhythmic drugs in patients with ventricular tachyarrhythmias. New Engl. J. Med. 329, 452–458.

Németh, M., Varro, A., Thormahlen, D., Papp, J.G., 1997. Tedisamil is a potent blocker of ATP-sensitive potassium channel in cardiac muscle. Exp. Clin. Cardiol. 2, 37–40.

Niu, X.W., Meech, R.W., 1998. The effect of polyamines on K_{ATP} channels in guinea-pig ventricular myocytes. J. Physiol. (London) 508 (2), 401–411.

Noma, A., 1983. ATP-regulated K^+ channels in cardiac muscle. Nature 305, 147–148.

Olschewski, A., Braü, M.E., Olschewski, H., Hemplemann, M.D., Vogel, W., 1996. ATP-dependent potassium channel in rat cardiomyocytes is blocked by lidocaine. Circulation 93, 656–659.

Opie, L.H., 1993. Modulation of ischemia by regulation of the ATP-sensitive potassium channel. Cardiovasc. Drugs Ther. 7, 507–513.

Sakuta, H., Okamoto, K., Watanabe, Y., 1992. Blockade by antiarrhythmic drugs of glibenclamide-sensitive K^+ channels in Xenopus oocytes. Br. J. Pharmacol. 107, 1061–1067.

Sato, T., Wu, B., Nakamura, S., Kiyosue, T., Arita, M., 1993. Cibenzoline inhibits diazoxide- and 2,4-dinitrophenol-activated ATP-sensitive K^+ channels in guinea-pig ventricular cells. Br. J. Pharmacol. 108, 549–556.

Sato, T., Shigematsu, S., Arita, M., 1995. Mexiletine-induced shortening of the action potential duration of ventricular muscles by activation of ATP-sensitive K^+ channels. Br. J. Pharmacol. 115, 381–382.

Shigematsu, S., Arita, M., 1997. Anoxia-induced activation of ATP-sensitive K+ channels in guinea pig ventricular cells and its modulation by glycolysis. Cardiovasc. Res. 35, 273–282.

Slawsky, M.T., Castle, N.A., 1994. K^+ channel blocking actions of flecainide compared with those of propafenone and quinidine in adult rat ventricular myocytes. J. Pharmacol. Exp. Ther. 269, 66–74.

Schoenmakers, T.J.M., Visser, G.J., Flik, G., Theuvenet, A.P.R., 1992. CHELATOR: an improved method for computing metal ion concentrations in physiological solutions. Biotechniques 12 (6), 870–879.

Spinelli, W., Sorota, S., Siegal, M., Hoffman, B.F., 1991. Antiarrhythmic actions of the ATP-regulated K^+ current activated by pinacidil. Circ. Res. 68, 1127–1137.

Spitzer, K.W., Bridge, J.H.B., 1989. A simple device for rapidly exchanging solution surrounding a single cardiac cell. Am. J. Physiol. 256, C441–C447.

Takano, M., Noma, A., 1993. The ATP-sensitive K^+ channel. Prog. Neurobiol. 41, 21–30.

Tebbakh, H., Forrat, R., Simurdova, M., Simurda, J., Christé, G., 1997. Propafenone is a pure blocker of rabbit cardiac ATP_i-sensitive K current. J. Mol. Cell. Cardiol. 29, A120, (Abstract).

Tomai, F., Crea, F., Gaspardone, A., Versaci, F., Depaulis, R., Penta de Peppo, A., Chiarello, L., Gioffre, P.A., 1994. Ischemic preconditioning during coronary angioplasty is prevented by glibenclamide, a selective ATP-sensitive K^+ channel blocker. Circulation 90, 700–705.

Tourneur, Y., Marion, A., Gautier, P., 1994. SR47063, a potent channel opener, activates K_{ATP} and a time-dependent current likely due to potassium accumulation. J. Membr. Biol. 142, 337–347.

Veldkamp, M.W., van Ginneken, A.C.G., Bouman, L.N., Opthof, T., 1995. ATP-sensitive K^+ channels have lower density in human than in rabbit ventricular myocyte. Eur. Heart J. 16, 367, Abstract.

Verkerk, A.O., Veldkamp, M.W., Van Ginneken, A.C.G., Bouman, L.N., 1996. Biphasic response of action potential duration to metabolic inhibition in rabbit and human ventricular myocytes: role of transient outward current and ATP-regulated potassium current. J. Mol. Cell. Cardiol. 28, 2443–2456.

West, P.D., Bursill, J.A., Wyse, K.R., Marin, D.K., Campbell, T.J., 1996. Effect of the class III antiarrhythmic agent E-4031 on the ATP-sensitive potassium channel in rabbit ventricular myocytes. Pharmacol. Toxicol. 78, 89–93.

Wu, B., Sato, T., Kiyosue, T., Arita, M., 1992. Blockade of 2,4-dinitrophenol induced ATP sensitive potassium current in guinea-pig ventricular myocytes by class I antiarrhythmic drugs. Cardiovasc. Res. 26, 1095–1101.

Yasui, K., Anno, T., Kamiya, K., Boyett, M.R., Kodama, I., Toyama, J., 1993. Contribution of potassium accumulation in narrow extracellular spaces to the genesis of nicorandil-induced large inward tail current in guinea-pig ventricular cells. Pflügers Arch. 422, 371–379.